The ISME Journal (2012) 6, 1222–1237

www.nature.com/ismej

ORIGINAL ARTICLE

Microbial diversity of biofilm communities in microniches associated with the didemnid ascidian *Lissoclinum patella*

Lars Behrendt[1,2], Anthony WD Larkum[3], Erik Trampe[1], Anders Norman[2], Søren J Sørensen[2] and Michael Kühl[1,3,4]

[1]*Marine Biological Section, Department of Biology, University of Copenhagen, Helsingør, Denmark;* [2]*Section of Microbiology, Department of Biology, University of Copenhagen, Copenhagen, Denmark;* [3]*Plant Functional Biology and Climate Change Cluster, Department of Environmental Science, University of Technology Sydney, Sydney, New South Wales, Australia and* [4]*Singapore Center for Environmental Life Sciences Engineering, School of Biological Sciences, Nanyang Technological University, Singapore*

We assessed the microbial diversity and microenvironmental niche characteristics in the didemnid ascidian *Lissoclinum patella* using *16S rRNA* gene sequencing, microsensor and imaging techniques. *L. patella* harbors three distinct microbial communities spatially separated by few millimeters of tunic tissue: (i) a biofilm on its upper surface exposed to high irradiance and O_2 levels, (ii) a cloacal cavity dominated by the prochlorophyte *Prochloron* spp. characterized by strong depletion of visible light and a dynamic chemical microenvironment ranging from hyperoxia in light to anoxia in darkness and (iii) a biofilm covering the underside of the animal, where light is depleted of visible wavelengths and enriched in near-infrared radiation (NIR). Variable chlorophyll fluorescence imaging demonstrated photosynthetic activity, and hyperspectral imaging revealed a diversity of photopigments in all microhabitats. Amplicon sequencing revealed the dominance of cyanobacteria in all three layers. Sequences representing the chlorophyll *d* containing cyanobacterium *Acaryochloris marina* and anoxygenic phototrophs were abundant on the underside of the ascidian in shallow waters but declined in deeper waters. This depth dependency was supported by a negative correlation between *A. marina* abundance and collection depth, explained by the increased attenuation of NIR as a function of water depth. The combination of microenvironmental analysis and fine-scale sampling techniques used in this investigation gives valuable first insights into the distribution, abundance and diversity of bacterial communities associated with tropical ascidians. In particular, we show that microenvironments and microbial diversity can vary significantly over scales of a few millimeters in such habitats; which is information easily lost by bulk sampling.

The ISME Journal (2012) **6,** 1222–1237; doi:10.1038/ismej.2011.181; published online 1 December 2011
Subject Category: microbial ecology and functional diversity of natural habitats
Keywords: *Acaryochloris marina*; *Lissoclinum patella*; microenvironment; microbial diversity; microsensor; *Prochloron*

Introduction

Marine microbes are pivotal players in food webs, primary production and biogeochemical cycling (Samuel, 2000). The biodiversity of marine microbial communities has been under close investigation using culturing, ribotyping and, more recently, massive parallel pyrosequencing of the *16S rRNA* gene or metagenomic surveys of bulk DNA extracted from the respective environments. Despite rapid accumulation of such sequence data, the extent of marine microbial biodiversity is still barely known (Pedrós-Alió, 2006), and uncultured bacteria composing the 'rare biosphere' are steadily accumulating (Sogin *et al.*, 2006); although criticism concerning a technical overestimation of species diversity has been growing accordingly (Reeder and Knight, 2009; Kunin *et al.*, 2010).

In recent years, the microbial diversity associated with sponges and other marine invertebrates has been under intense investigation, in part due to a prevalence of bioactive compounds in such organisms, with potential use in applied sciences (Taylor *et al.*, 2007, 2011; Menezes *et al.*, 2010; Thomas *et al.*, 2010; Webster and Taylor, 2011). In addition to marine sponges, didemnid ascidians present an interesting environment for the investigation of

Correspondence: L Behrendt, Marine Biological Section, Department of Biology, University of Copenhagen, Strandpromenaden 5, Helsingør DK-3000, Denmark.
E-mail: lbehrendt@bio.ku.dk
Received 6 September 2011; revised 1 November 2011; accepted 3 November 2011; published online 1 December 2011

symbiotic relationships (Adams, 2002; Hirose and Maruyama, 2004) and the discovery of new bioactive compounds (Sings and Rinehart, 1996; Ogi *et al.*, 2009; Erwin *et al.*, 2010). The role and importance of ascidian-associated microbes versus the host as a source of such secondary metabolites remains largely unexplored. For example, Schmidt *et al.* (2005) reported the production of bioactive cyclic peptides, patellamides, in the symbiotic prochlorophytic cyanobacterium *Prochloron* spp., which is found in large quantities within the cloacal cavity of the didemnid ascidian *Lissoclinum patella* (Schmidt *et al.*, 2005), whereas others have reported patellamide production in *L. patella* itself (Degnan *et al.*, 1989; Sings and Rinehart, 1996; Salomon and Faulkner, 2002). Another unique cyanobacterium, *Acaryochloris marina*, grows in biofilms on the underside of didemnid ascidians, where it uses chlorophyll (Chl) *d* to sustain its photosynthesis using near-infrared radiation (NIR; Kühl *et al.*, 2005). The *A. marina* type strain MBIC11017, originally isolated from *L. patella*, was hereafter sequenced and revealed a genome of unusually large size (Swingley *et al.*, 2008). The relative abundance of *A. marina* in these epizoic microbial communities remains unknown and besides a recent genomic survey focusing on *Prochloron*, and its secondary metabolism (Donia *et al.*, 2011), no further efforts have been made in studying the microbial diversity in *L. patella*.

Most surveys of microbial diversity are based on bulk sample analysis, with only few or missing metadata on the environmental characteristics of the sampled habitat. Thus, they lack key information about niche-defining physicochemical factors shaping the microbial assemblages. This is particularly critical when analyzing surface-associated microbial communities, where several studies of microbial mats (Ward *et al.*, 2006; Kunin *et al.*, 2008) and sediments (Lüdemann *et al.*, 2000; Böer *et al.*, 2009) have shown strong shifts in microbial communities along biogeochemical gradients over minute spatial scales. Although microenvironmental analysis of corals (Kühl *et al.*, 1995), sponges (Hanna *et al.*, 2005; Hoffmann *et al.*, 2008) and ascidians (Kühl and Larkum, 2002; Kühl *et al.*, 2005) have shown steep and dynamic microenvironmental conditions similar to biofilms and microbial mats, we are not aware of previous studies simultaneously mapping microbial diversity and fine-scale microenvironmental conditions in such organisms.

In this study, we employ a rare combination of molecular analysis, microscopic imaging and microsensor analysis to describe the microenvironments and microbial communities associated with *L. patella*. Microbial communities were sampled from three different microhabitats growing (i) on the high light-exposed surface of *L. patella*, (ii) inside the cloacal cavity of the ascidian and (iii) on the underside of *L. patella*. The microbial diversity was investigated by *16S rRNA* gene sequencing. In addition to such molecular data, we present the very first description of the O_2 and light microenvironment and the distribution of photopigments and photosynthetic activity across the investigated microhabitats associated with *L. patella*.

Materials and methods

More detailed information on Materials and methods are given in the Supplementary Online Materials.

Origin, preparation and transport of samples. Intact specimens (5–10 cm^2) of 5–10 mm thick *L. patella* were sampled at low tide ($\sim$2.8 m tidal range) from three different depths on the outer reef flat and crest off Heron Island (Figure 1; S23°26′055, E151°55′850): (i) 2.5–3.5 m (hereafter 'deep'), (ii) 1.5–2.5 m (hereafter 'intermediate') and (iii) 30 cm (hereafter 'shallow'). Specimens were kept in a shaded aquarium (<200 μmol photons m^{-2} s^{-1}) with a continuous supply of fresh seawater (26–28 °C) before subsampling. Relatively flat and homogeneous pieces of *L. patella* with a surface area of $\sim 2 \times 2$ cm were cut with a scalpel and immediately rinsed and submerged in filtered seawater. Cross-sections were cut from homogenous pieces with a razor blade for subsequent imaging. For DNA analysis, three independent biological replicates were collected at the shallow and deep site, whereas two replicates were collected at intermediate depths. From each of these replicates, three microbial consortia were sampled: (i) the upper surface layer, (ii) the underside of *L. patella*, both of which were collected using a sterilized razorblade, and (iii) the middle section containing the cloacal cavity harboring the deep green *Prochloron* spp. symbiont, which was collected using a pipette and gentle squeezing. This sampling design resulted in a total of 24 samples, which were used in DNA analysis. Samples used for subsequent DNA extraction were immediately submerged in RNAlater (Ambion, Applied Biosystems, Foster City, CA, USA), incubated in a refrigerator overnight and then frozen at −80 °C the next morning. These samples were transported back to the laboratory on dry ice and stored at −80 °C upon arrival.

Microsensor measurements. An intact specimen of *L. patella* was used for measuring the depth distribution of O_2 and spectral scalar irradiance with optical and electrochemical microsensors. Scalar irradiance measurements were performed using a fiber-optic scalar irradiance microprobe mounted onto a motorized micromanipulator system (Unisense, Aarhus, Denmark) and connected to a spectrometer (QE65000, Ocean Optics, Dunedin, FL, USA; Kühl, 2005). The scalar microprobe was inserted in 0.2-mm steps into *L. patella* and the measured spectra were normalized to the spectral downwelling irradiance as determined from a black non-reflective beaker. Samples were irradiated

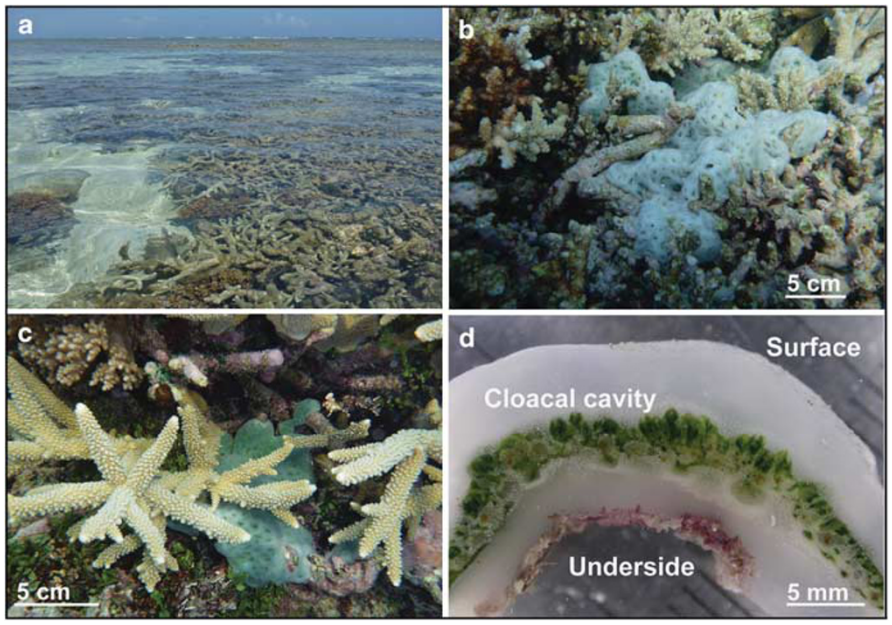

Figure 1 The tropical didemnid ascidian *L. patella* in its natural habitat. (**a**) Inner coral reef crest at low tide on Heron Island, QLD, Australia. (**b**) Specimen of *L. patella* found nested within dead and living coral branches. (**c**) Deep-green specimen of *L. patella*, where the green coloration originates from its obligate symbiont *Prochloron* spp. that resides in the cloacal cavities of the ascidian. (**d**) Cross-section of *L. patella*. Note the thick reddish biofilm covering the underside of the tunic and the green *Prochloron* cells in the cloacal cavity of the ascidian. 'Surface', 'cloacal cavity' and 'underside' denote the sites were samples were taken for subsequent analysis in this study.

vertically from above with a fiber-optic tungsten halogen lamp (KL-2500, Schott, Mainz, Germany). Oxygen microsensors (OX25 and OX50, Unisense) were connected to a multimeter and mounted onto the same micromanipulator system as described above. Data acquisition and sensor positioning during microprofiling of scalar irradiance or O_2 concentration was performed using dedicated software (SensorTrace Pro, Unisense).

Hyperspectral imaging. The surface and underside of precut 2×2 cm pieces of ascidian tissue were imaged using a dissection microscope (SZ X16, Olympus, Tokyo, Japan) equipped with a hyperspectral image scan unit (100T-VNIR, Themis Vision, Bay Saint Louis, MS, USA). Hyperspectral image stacks were corrected (in *Hypervisual* 3.0, Themis Vision) to percent (%) reflectance using reflectance standards (Spectralon, Labsphere, North Sutton, NH, USA) and corrected for background noise under darkness. Normalized hyperspectral image stacks were processed according to Polerecky *et al*. (2009) and are presented in false color, quantifying the light attenuation around 710 nm (Chl *d*), 675 nm (Chl *a*; Figure 2c) and 560 nm (phycoerythrin; Figure 2d).

Variable chlorophyll fluorescence imaging. The photosynthetic activity of biofilms on the underside and the surface of the tunic of *L. patella*, respectively, were monitored by variable chlorophyll fluorescence imaging using a pulse-amplitude-modulated imaging system (I-PAM, Walz GmbH, Effeltrich, Germany) using blue light-emitting diodes (470 nm) for measuring and actinic light. Blue measuring light is efficient in monitoring the photosynthetic activity of the NIR-absorbing *A. marina*, due to the Chl *d* Soret band absorption at 460–470 nm. Pulse-amplitude-modulated chlorophyll fluorescence imaging systems have been described in detail elsewhere (Schreiber, 2004; Kühl and Polerecky, 2008; Trampe *et al.*, 2011).

Molecular analysis

DNA extraction. Biofilms from the underside and the surface, stored in RNAlater (Ambion, Applied Biosystems), were flash frozen in liquid nitrogen and then crushed in precleaned and sterilized mortars. The resulting powder was immediately processed using the standard FastDNA for soil kit (Qbiogene, Illkirch, France), with two additional bead-beating cycles. Samples from the cloacal cavity of *L. patella* were directly used in the bead-beating process but otherwise treated the same way as the other two samples. Between bead-beating cycles, the samples were cooled on ice for 2 min. The resulting DNA was eluted in TAE buffer and the DNA was quantified using a Qubit-fluorometer (Invitrogen, Carlsbad, CA, USA), checked for integrity on a 0.8% agarose gel and stored at $-20\,^{\circ}$C until further use.

PCR amplification and pyrosequencing. Tag-encoded *16S rRNA* gene (= amplicon) pyrosequencing was performed on DNA extracted from a total of 24 samples, encompassing the three biofilms (surface,

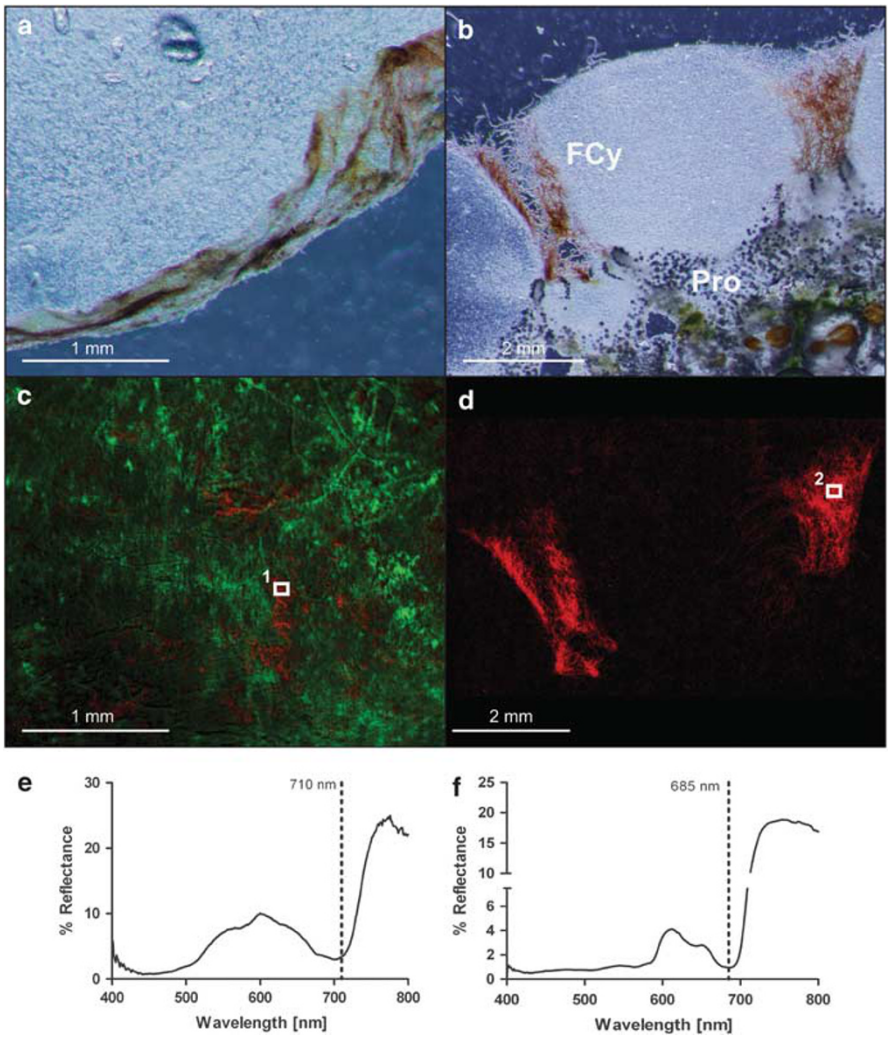

Figure 2 (**a**) Typical biofilm found on the underside of the tropical ascidian *L. patella*. (**b**) Cross-section of the same ascidian showing filamentous cyanobacteria (FCy) on the surface, part of the cloacal cavity containing green *Prochloron* cells (Pro) and the animal zooid. (**c**) Color-coded composite images of hyperspectral image stacks taken from the biofilm displayed in **a**, red quantifies the absorption at 710 nm (specific for Chl *d*), whereas green quantifies absorption at 675 nm (specific for Chl *a*). (**d**) Hyperspectral composite images color coded to quantify absorption at 560 nm (specific for phycoerythrin); images were taken from the same biofilm as displayed in **b**. The numbers in both **c** and **d** denote specific areas of interest, exhibiting the reflectance spectra shown in **e** and **f**.

cloacal cavity and underside) sampled at the shallow and deep sites (three replicates each) or at intermediate depths (two replicates each). The DNA concentration in all samples was adjusted to 5 ng/μl using molecular biology grade water. A 466-bp fragment of the *16S rRNA* gene was amplified using the primers 341F (5-CCTAYGGGRBGCASCAG-3) and 806R (5-GGACTACNNGGGTATCTAAT-3) flanking the V3 and V4 regions (Youngseob *et al.*, 2005). PCR amplification was performed using the Phusion Hot Start DNA Polymerase (Finnzymes Oy, Espoo, Finland) with the following cycle conditions: 98 °C for 30 s, followed by 35 cycles of 98 °C for 5 s, 56 °C for 20 s and 72 °C for 20 s and a final extension of 72 °C for 5 min. After PCR amplification, the samples were held at 70 °C for 3 min and were then moved on ice, preventing hybridization between PCR products and nonspecific amplicons. PCR products were separated on a 1% agarose gel and purified using the Montage Gel extraction kit (Millipore, Billerica, MA, USA). A second round of PCR was performed as described above, except that this time primers with adapters and tags were used (Holmsgaard *et al.*, 2011) and the number of cycles was reduced to 15. After further gel purification and quantification using a Qubit-fluorometer (Invitrogen) the amplified fragments were mixed in equal concentrations and sequenced on one of two regions of a 70–75 GS PicoTiterPlate using a GS-FLX pyrosequencing system (Roche, Basel, Switzerland).

Sequence analysis and visualization. A total of 182.375 amplicon sequence reads were obtained from pyrosequencing. After quality filtering, 161.499 sequences were left for further sequence analysis using the QIIME software package (QIIME, version 1.2.1, http://qiime.sourceforge.net/). Phylotyping was performed by picking representatives

from each operational taxonomic unit (OTU) and aligning them against a V3/V4-truncated core alignment of the Greengenes database (http://greengenes.lbl.gov). All OTUs identified as chloroplasts were subsequently removed from the OTU table, reducing the total number of sequences in the data set to 140.871. In order to present a succinct overview of the major taxonomic groups OTUs summing to >100 sequences across all samples were used for further $\log_{10}+1$ transformation and visualization in a heatmap using the taxonomy assignments described. The same subset of OTUs was used for metabolic assignments, based on a thorough literature search of conserved key properties within major taxonomic groups.

Results

Overall distribution of biofilms and pigmented cells
Distinct pigmented bacterial biofilms covered the underside and the surface of the tropical didemnid ascidian *L. patella*, while large amounts of green symbiotic *Prochloron* cells were contained within the cloacal cavity of the animal (Figures 1d and 2).

Photopigment distribution
Ascidians collected at intermediate depths were imaged using light and fluorescence microscopy and depicted green-yellowish biofilms on the underside (Figure 2a) and clusters of red filamentous cyanobacteria in the opening of the cloacal cavity of the animal surrounded by a thin biofilm on the surrounding upper surface of the *L. patella* tunic (Figure 2b). *Prochloron* cells were abundant in the cloacal cavity of all collected specimens of *L. patella* forming a deep-green layer (Figures 1d and 2b). Hyperspectral imaging revealed photopigments absorbing light in the NIR, typical for Chl *d* on the underside of *L. patella* (Figure 2c; absorptivity at 710 nm displayed in red) mixed with photopigments with absorption characteristics typical for Chl *a* (Figure 2c; absorptivity at 675 nm displayed in green). Surface-associated filamentous bacteria on the upper surface of *L. patella* showed absorbance distinctive for phycoerythrin (Figure 2d; absorptivity at 560 nm displayed in red) as well as Chl *a* (Figure 2f). Reflectance spectra of distinct areas of interest on the underside (Figure 2e) and the surface (Figure 2f) biofilms showed reflectance minima around 710 nm (Chl *d* specific) and 675 nm (Chl *a*), respectively.

Light and O_2 microenvironments in L. patella
A scalar irradiance probe was inserted into an intact specimen of *L. patella* to capture qualitative and quantitative changes in light distribution throughout the three microhabitats. Measurements just below the surface of *L. patella* indicated a local increase in scalar irradiance up to 216% due to intense scattering in the upper tunic (red line; Figure 3c). Light in the cloacal cavity of *L. patella* (green line; Figure 3c) was reduced by an order of magnitude in the blue and red part of the spectrum when compared with subsurface measurements. Absorption signatures of chlorophylls (Chl *a* 440/675 nm and Chl *b* ~453/642 nm), bacteriochlorophyll (Bchl *a* 805/830–890 nm) and phycobiliproteins (phycoerythrin ~560 nm and phycocyanin ~620–630 nm) were present in both the cloacal cavity containing *Prochloron* cells as well as in the biofilm covering the underside of the ascidian. Light reaching the underside of the ascidian (blue line; Figure 3c) was enriched in NIR (>700 nm), whereas visible wavelengths were further depleted in intensity to ~0.1–1% of the incident irradiance.

We captured the temporal and spatial O_2 distribution in *L. patella* by performing stepwise O_2 measurements under light and in darkness. During darkness, anoxic conditions prevailed below a depth of ~0.8–1 mm, whereas the surface layer of the tunic remained well oxygenated under dark conditions. During light conditions, we observed a strong O_2 uptake in the upper tunic, whereas O_2 concentrations increased stepwise to a maximum of ~250% air saturation within the cloacal cavity of *L. patella* under an incident irradiance of 1350 μmol photons $m^{-2}\,s^{-1}$ at its surface. Experimental light–dark shifts with the O_2 microsensor tip positioned in the cloacal cavity of *L. patella* showed a rapid O_2 depletion immediately after onset of darkness (data not shown). No O_2 measurements were performed in deeper layers due to risk of breaking the fragile glass microelectrode.

Photosynthetic activity of phototrophic biofilms
Photosynthetic activity was measured as the relative electron transport rate (rETR) versus quantum irradiance for all three biofilm communities associated with *L. patella* (Figure 3d). At an irradiance of ~1000 μmol photons $m^{-2}\,s^{-1}$, the highest photosynthetic activity was found in the *Prochloron*-rich middle section of *L. patella* (rETR >19); under the same irradiance the biofilm on the underside of *L. patella* exhibited a rETR of ~6. The rETR versus quantum irradiance curve of surface-associated filamentous bacteria increased steeply, reaching a rETR of ~13 and then dropped to 0 at photon concentrations in excess of 324 μmol $m^{-2}\,s^{-1}$. Phototrophic bacteria on the underside reached light saturation at ~400 μmol photons $m^{-2}\,s^{-1}$, whereas cells in the cloacal cavity of *L. patella* were not saturated at the maximum irradiance employed in our PAM measurements (1000 μmol photons $m^2\,s^{-1}$).

Microbial diversity of biofilms associated with L. patella
The microbial diversity of 24 individual samples was evaluated using *16S rRNA* gene sequencing. All three biofilm communities were sampled along a gradient ranging from the outer slope of the reef

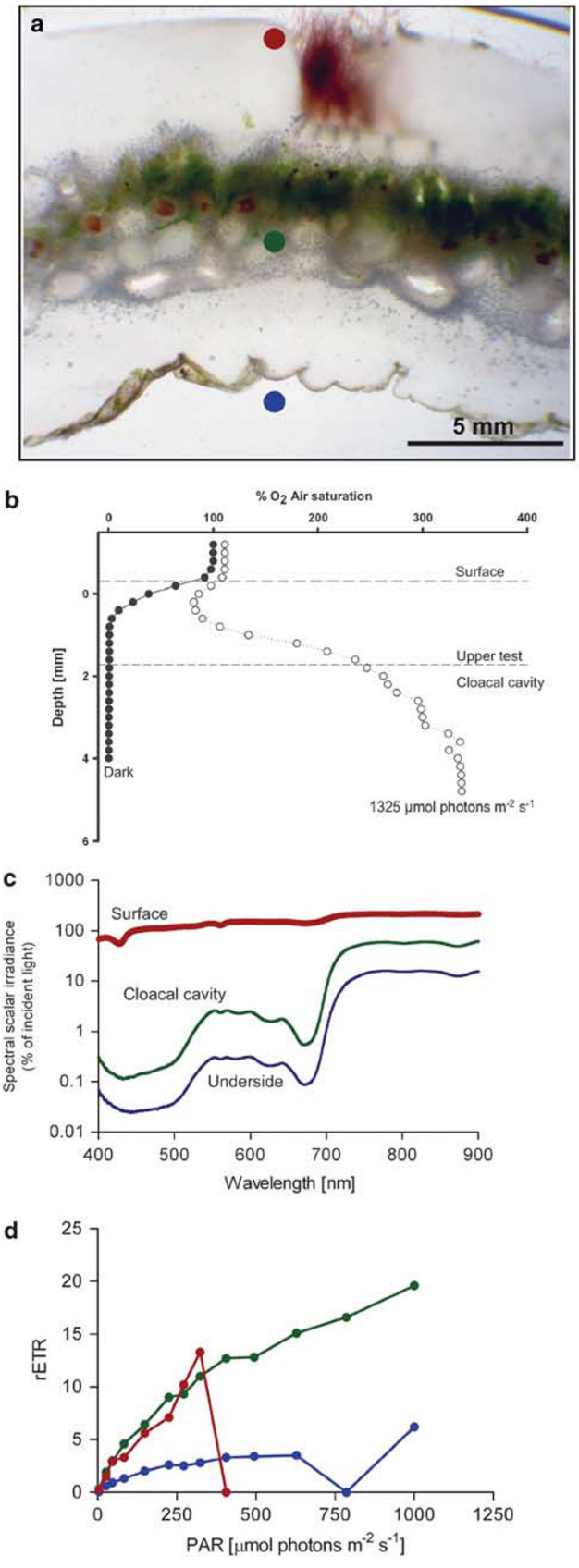

crest (depth ~2.5–3.5 m), the reef crest itself (depth ~1.5–2.5 m) to the inner reef flat (depth 0.3–1 m). The top 10 dominating OTUs and their taxonomic assignments on the phylum level are shown in Table 1. All samples across depth gradients and throughout the three different biofilm communities were dominated by sequences related to the phyla *Cyanobacteria* and *Proteobacteria*. Sequences from the tunic surface were mostly associated with *Cyanobacteria*, which were most common in the deep site (80%) and became lower in numbers with decreasing depth, reaching >60% at the intermediate site and ~20% at the shallow site (see also Supplementary Figure S1). *Proteobacteria*-associated sequences on the surface biofilm followed the opposite trend and increased with decreasing depth. Other abundant sequences from the surface samples were related to *Bacteroidetes*, *Verrucomicrobia* and *Fusobacteria*.

Sequence reads retrieved from the cloacal cavity of *L. patella* were mostly assigned to the phylum *Cyanobacteria* (about 68–90% for the three depths), whereas the second most abundant phylum was *Proteobacteria* (7–25%). Less abundant phyla in the cloacal cavity included *Bacteroidetes*, *Fusobacteria* and the candidate phylum *OP8*. Cyanobacterial sequences were also abundant on the underside of the ascidian and their contribution remained relatively constant across depths (45–58%); the same was true for sequences related to *Proteobacteria* (20–27%) and *Bacteroidetes* (12–20%). In addition to these three phyla, the biofilms on the underside contained sequences associated with *Verrucomicrobia*, *Chloroflexi* and *Actinobacteria*.

Clustering of the most abundant bacterial OTUs in a heatmap

In order to display clustering of OTUs in a succinct way, only OTUs containing a total of >100 sequences across all samples were $\log_{10}+1$ transformed and subsequently clustered in a heatmap (Figure 4). Visually, the microbial diversity presented in Table 1 is reflected in the heatmap.

Figure 3 Microenvironments and photosynthetic activity in *L. patella* and its associated biofilm communities. (**a**) Cross-section of *L. patella*. Colored dots indicate the different layers of the animal, where measurements where performed. Red denotes measurements taken just below the surface, green just below the cloacal cavity, and blue just below the underside of the ascidian. (**b**) Oxygen concentration gradients measured through an intact specimen of *L. patella* in darkness or under an irradiance of 1350 µmol photons m^{-2} s^{-1}. The upper surface of the tunic and the boundary toward the cloacal cavity are indicated by the two horizontal lines. (**c**) Spectral scalar irradiance (in percent (%) of incident irradiance at the tunic surface) as measured with a fiber-optic microprobe just below the three different compartments within *L. patella*. Color coding is the same as in **a**. (**d**) Photosynthetic activity measured as the photosystem II-related rETR versus irradiance in the three different biofilms.

Table 1 Classification of the 10 most abundant phyla for the three sampling depths and microhabitats associated with *Lissoclinum patella*

Deep		*Intermediate*		*Shallow*	
Surface					
Cyanobacteria	80.19 ± 24.14	Cyanobacteria	61.55 ± 42.3	Proteobacteria	42.25 ± 8.24
Proteobacteria	9.75 ± 11.28	Proteobacteria	31.12 ± 33.8	Bacteroidetes	35.36 ± 3.30
Bacteroidetes	5.07 ± 5.45	Bacteroidetes	4.34 ± 5.04	Cyanobacteria	20.53 ± 11.0
Verrucomicrobia	4.08 ± 6.30	Fusobacteria	1.66 ± 2.07	Verrucomicrobia	1.22 ± 1.61
Fusobacteria	0.32 ± 0.46	Verrucomicrobia	0.77 ± 0.85	OP8	0.15 ± 0.13
GN02	0.16 ± 0.23	GN02	0.33 ± 0.39	Actinobacteria	0.10 ± 0.06
Actinobacteria	0.08 ± 0.14	Firmicutes	0.11 ± 0.09	Planctomycetes	0.09 ± 0.14
Planctomycetes	0.07 ± 0.08	Planctomycetes	0.03 ± 0.01	Firmicutes	0.08 ± 0.06
Firmicutes	0.06 ± 0.07	OP8	0.01 ± 0.02	ZB2	0.05 ± 0.09
Acidobacteria	0.03 ± 0.03	ZB2	0.01 ± 0.02	Fusobacteria	0.05 ± 0.08
Cloacal cavity					
Cyanobacteria	89.89 ± 3.85	Cyanobacteria	67.94 ± 18.8	Cyanobacteria	80.92 ± 2.39
Proteobacteria	7.63 ± 2.84	Proteobacteria	24.96 ± 11.7	Proteobacteria	12.55 ± 3.86
Bacteroidetes	0.81 ± 0.21	Fusobacteria	4.83 ± 1.24	OP8	3.54 ± 1.73
OP8	0.75 ± 0.53	Bacteroidetes	1.50 ± 0.07	Bacteroidetes	1.38 ± 0.08
Fusobacteria	0.43 ± 0.62	OP8	0.46 ± 6.14	Verrucomicrobia	0.62 ± 0.25
Firmicutes	0.21 ± 0.23	Firmicutes	0.10 ± 0.12	Firmicutes	0.60 ± 0.78
Verrucomicrobia	0.14 ± 0.06	Actinobacteria	0.09 ± 0.05	Actinobacteria	0.29 ± 0.36
Actinobacteria	0.08 ± 0.07	Verrucomicrobia	0.05 ± 0.05	No blast hit	0.03 ± 0.02
Lentisphaerae	0.03 ± 0.05	Spirochaetes	0.04 ± 0.03	Spirochaetes	0.03 ± 0.02
Spirochaetes	0.02 ± 0.02	Lentisphaerae	0.01 ± 0.02	GN02	0.01 ± 0.01
Underside					
Cyanobacteria	46.90 ± 8.00	Proteobacteria	45.02 ± 11.4	Cyanobacteria	58.53 ± 2.01
Proteobacteria	24.75 ± 5.90	Cyanobacteria	27.00 ± 7.58	Proteobacteria	20.65 ± 0.73
Bacteroidetes	16.36 ± 4.74	Bacteroidetes	19.35 ± 1.43	Bacteroidetes	12.77 ± 3.07
Verrucomicrobia	6.29 ± 3.30	Verrucomicrobia	3.30 ± 0.27	Verrucomicrobia	4.10 ± 0.97
Chloroflexi	1.94 ± 0.41	Actinobacteria	1.63 ± 1.22	Chloroflexi	0.97 ± 0.20
Actinobacteria	0.89 ± 0.19	Acidobacteria	0.84 ± 0.49	Actinobacteria	0.71 ± 0.24
Acidobacteria	0.87 ± 0.39	Chloroflexi	0.79 ± 0.56	Planctomycetes	0.67 ± 0.27
Planctomycetes	0.63 ± 0.45	Planctomycetes	0.61 ± 0.30	Acidobacteria	0.60 ± 0.12
SBR1093	0.20 ± 0.23	WS3	0.18 ± 0.23	ZB2	0.16 ± 0.16
WS3	0.18 ± 0.14	GN02	0.17 ± 0.18	WPS-2	0.13 ± 0.02

Relative percentages of OTUs and their respective standard deviation from the mean are based on two (intermediate depth) or three (deep and shallow site) independent biological replicates. Chloroplast sequences were removed, whereas Archeal sequences were included in the analysis.

Samples taken from the underside showed a high diversity, as reflected in the amount of OTUs and their relative abundance, while a lower diversity was found in biofilms originating from the surface and the cloacal cavity. Euclidean distance analysis revealed four distinct clusters, which were color coded and labeled numerically. Cluster I (light blue) contains samples taken at all three depths originating from the underside of *L. patella*. Cluster II (green) encompasses only samples taken from the cloacal cavity (=*Prochloron*) from all three depths. Cluster III (yellow) is nested within cluster II and contains three surface samples, which were all sampled at shallow depths and are dominated by OTUs taxonomically assigned to *Flammeovirgaceae* and *Kiloniella* spp., both of which are less pronounced in other surface samples taken at deeper depths. Cluster IV (red) contains the remaining surface samples from the intermediate and deep site and a single sample from the cloacal cavity (intermediate depth). Within these clusters, the most frequent OTUs belong to: cluster (I) *Azospirillum brasilense, A. marina, Symploca* spp. and the family *Flammeovirgaceae*; cluster (II) *Prochloron*, *Kiloniella* spp., *Rhodospirillaceae, Vibrio* spp. and *HMMVPog-54*; cluster (III) *Kiloniella*, *Flammeovirgaceae* and *Planktothricoides*; and cluster (IV) *Planktothricoides* spp., *Kiloniella* and *Flammeovirgaceae.*

Estimation of microbial richness and diversity

The complexity and richness of communities can be simplified and expressed by nonparametric estimators, providing a way to compare complex communities with each other and estimate the completeness of sampling (Schloss and Handelsman, 2005). Species richness is frequently measured as the number of OTUs present in a sample and is in this study given as the chao1 and abundance based-coverage estimator. Species diversity takes into account the evenness of the OTU distribution and is commonly expressed in the form of the Shannon index (*H*). Read libraries were rarefied to accommodate for the lowest number of reads found in our data set (=4009, see Supplementary Table 1) and

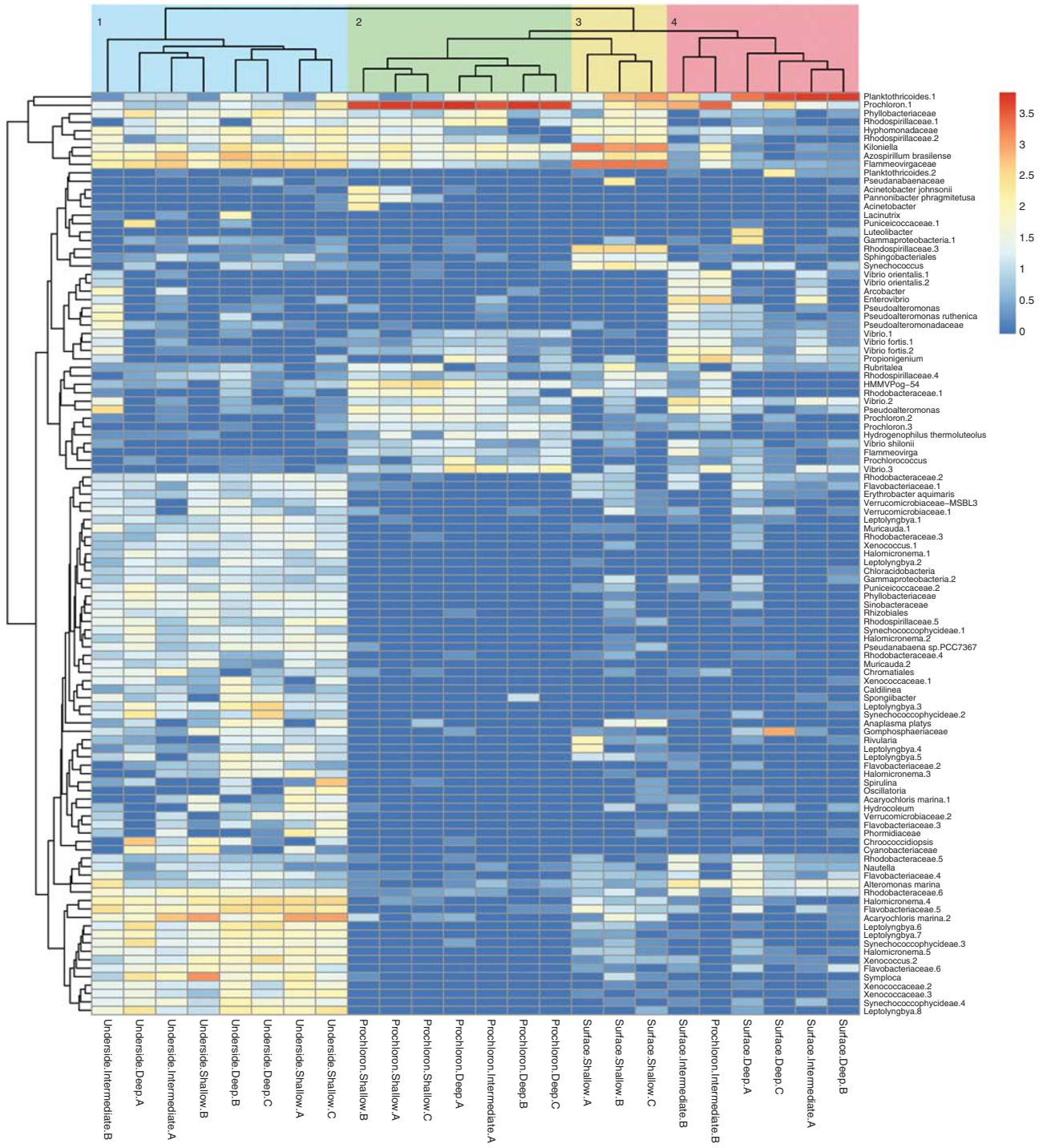

Figure 4 Heatmap of *16S rRNA* gene sequences obtained from bacterial biofilms associated with the underside, the surface or the cloacal cavity (=*Prochloron*) of *L. patella*, respectively. Independent biological replicates of the sampled biofilms are labeled sequentially, that is, 'Surface.deep.A–C' indicating three replicates. The three sampling depths are indicated after the name of the biofilm and denote the 'deep' (2.5–3.5 m), 'intermediate' (1.5–2.5 m) and 'shallow' site (0.3–1 m). Only OTUs with a sum of >100 assigned sequences across all samples were used for further $\log_{10}+1$ transformation. Taxonomy was assigned to OTU representatives using best Blast hits against the Greengenes database. Duplicate OTUs were numbered sequentially for clarification. OTU clustering is shown along the *y* axis; dendrogram distances are based upon relative abundances within the data matrix and not on phylogenetic relationships. The top dendrogram is based on Euclidean distances and represents clustering into four distinct clusters (1–4) according to relative abundances within the data matrix. Cluster I (light blue) contains all samples originating from the underside of the ascidian, and cluster II (green) contains all samples taken from the cloacal cavity (=*Prochloron*), except one. Cluster III (yellow) is nested within cluster II and contains three surface samples. Cluster IV (red) contains the remaining surface samples and the last sample taken from the cloacal cavity.

used for subsequent calculation of microbial richness and diversity estimators. The highest bacterial diversity was found in samples originating from the underside (*H* index = 6.58–7.22, see Table 2), whereas the lowest bacterial diversity occurred in samples taken from the cloacal cavity of *L. patella* (*H* index = 1.07–3.30). Diversity estimated by the Simpson index showed a similar pattern, with indices ranging from 0.19 (cloacal cavity) to 0.98 (underside). Richness estimates ranged from 167 to 1278 (chao1) and 176 to 1268 (abundance based-coverage estimator), with the lowest values found in the cloacal cavity of *L. patella* dominated by *Prochloron*, whereas the greatest richness was found in samples taken from the underside of *L. patella*.

Oxygen and carbon metabolism of L. patella*-associated microbes*

Taxonomic assignments displayed in the heatmap were used to determine the O_2 and carbon metabolism in the major bacterial OTUs; this was done by a thorough literature research identifying the key conserved properties for the dominating OTUs. This approach has some uncertainties but still provides a general overview of the metabolic functions in the associated biofilms. Phototrophic bacteria were generally abundant in the cloacal cavity, on the underside and the surface of *L. patella* (Supplementary Figure S2A). Sequences associated with chemotrophic bacteria seem to dominate the microbial community on the underside of *L. patella* at intermediate depths and surface biofilms at shallow depths. Sequences belonging to aerobic bacteria were commonly found in all three micro-environments (Supplementary Figure S2B), whereas facultative and obligate anaerobes were more often found in the cloacal cavity than on the surface or underside of the ascidian.

Principal component analysis of associated biofilm communities

Principal component analysis of the jackknifed-weighted UniFrac distances revealed two distinct clusters of characteristic communities found (i) on the underside and (ii) in the cloacal cavity of *L. patella* (Figure 5). Samples originating from the cloacal cavity clustered to the right of the primary axis (42.23% of the variation explained), whereas samples taken from the underside were found clustered to the left of the primary axis. Both samples taken from the underside and the cloacal cavity also cluster in the second dimension (25.43% of the variation explained). Samples taken from the surface formed a less stringent cluster and appeared somewhat related to bacterial communities found in the cloacal cavity. Three of the surface-associated

Table 2 Table of microbial diversity and richness estimators found throughout 24 samples

Sample ID	*Diversity estimator*		*Richness estimator*	
	Shannon	*Simpson*	*chao1*	*ACE*
LP28. Underside.Intermediate	7.22	0.98	988.30	1040.41
LP1. Underside.Deep	7.17	0.98	1121.06	1137.47
LP31. Underside.Shallow	6.98	0.97	1223.51	1319.05
LP2. Underside.Deep	6.98	0.98	873.28	966.39
LP25. Underside.Intermediate	6.90	0.96	1278.03	1305.35
LP4. Underside.Deep	6.86	0.97	1167.87	1194.77
LP34. Underside.Shallow	6.77	0.96	1204.41	1268.65
LP33. Underside.Shallow	6.58	0.94	1231.28	1249.61
LP28a. Surface.Intermediate	6.05	0.94	630.79	657.80
LP1a. Surface.Deep	5.09	0.81	933.90	985.68
LP33a. Surface.Shallow	4.39	0.86	676.26	715.08
LP34a. Surface.Shallow	3.60	0.82	449.14	477.48
LP31a. Surface.Shallow	3.51	0.76	478.13	491.34
LP28b. Cloacal cavity.Intermediate	3.30	0.71	316.57	327.37
LP33b. Cloacal cavity.Shallow	2.12	0.42	294.71	379.08
LP25b. Cloacal cavity.Intermediate	2.09	0.42	255.78	274.00
LP4a. Surface.Deep	1.98	0.48	307.79	358.87
LP31b. Cloacal cavity.Shallow	1.86	0.38	288.71	303.45
LP34b. Cloacal cavity.Shallow	1.76	0.36	272.13	294.92
LP1b. Cloacal cavity.Deep	1.70	0.33	187.03	204.52
LP2a. Surface.Deep	1.22	0.20	352.00	395.58
LP25a. Surface.Intermediate	1.19	0.21	257.50	292.19
LP4b. Cloacal cavity.Deep	1.09	0.21	187.40	197.22
LP2b. Cloacal cavity.Deep	1.07	0.19	167.43	176.76

Abbreviation: ACE, abundance based-coverage estimator.
These estimators were calculated on an OTU table rarefied to the lowest number of sequences in these 24 libraries (= 4009 reads). All OTUs taxonomically assigned as chloroplasts and Archaea were removed before analysis. The bacterial alpha-diversity is displayed by the Shannon and Simpson indices, whereas species richness is described by the chao1 and ACE estimators.

samples are located in the lower left of the graph, forming their own separate cluster. In combination, the two principal component analysis axes explained 67.6% of the variation between the different microbial communities on and within *L. patella*.

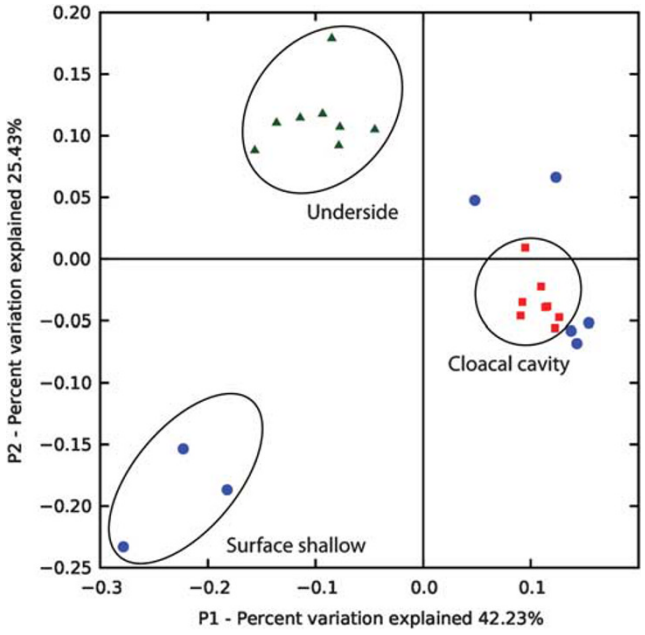

Figure 5 Principal component analysis of jackknifed-weighted UniFrac distances. Colors indicate the three different microhabitats sampled in *L. patella*; green triangles = underside; blue circles = surface; red squares = cloacal cavity.

Sequence abundance of phototrophic bacteria as a function of depth

Sequences assigned to bacterial groups known to contain photopigments (Bchl *a* and Chl *d*) absorbing near infrared radiation were used to determine a potential depth dependency in relative sequence abundance. Linear regression revealed a strong negative correlation between depth and the relative abundance of sequences belonging to the family *Rhodospirillaceae* ($R^2 = 0.882$, Figure 6a), *Rhodobacteraceae* ($R^2 = 0.757$, Figure 6c) and the cyanobacterium *A. marina* ($R^2 = 0.842$, Figure 6b). *Rhodospirillaceae*-associated sequences found on the surface of *L. patella* were much more abundant at shallow depths ($11.6 \pm 2.3\%$) than in intermediate ($0.13 \pm 0.14\%$) and deep waters ($0.18 \pm 0.14\%$). The same depth gradient was observed on the underside of *L. patella* for the Chl *d*-containing cyanobacterium *A. marina* (shallow = $14 \pm 0.9\%$, intermediate = $6.78 \pm 6.3\%$ and deep = $1.3 \pm 0.5\%$) and the purple bacteria *Rhodobacteraceae* within the cloacal cavity of the ascidian (shallow = $1.9 \pm 0.86\%$, intermediate = $0.59 \pm 0.05\%$ and deep = $0.25 \pm 0.13\%$). A less supported correlation ($R^2 = 0.234$, Figure 6d) was obtained for the bacteriochlorophyll containing

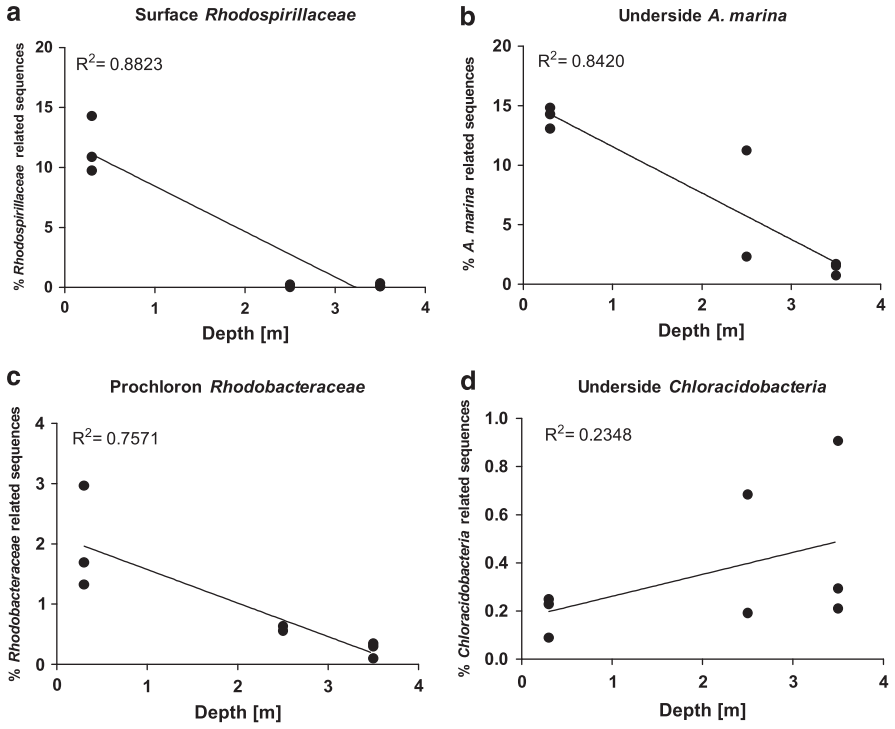

Figure 6 Percent of phototrophic bacteria-related OTUs versus sampling depth. The sum of several OTUs taxonomically assigned to either (**a**) *Rhodospirillaceae,* (**b**) *A. marina,* (**c**) *Rhodobacteraceae* or (**d**) *Chloracidobacteria* were calculated for each sampling site and depth. Two (intermediate depth) or three (shallow and deep site) biological replicates are displayed in the graph as individual points. The relative percentage of sequences was calculated for the biofilm sample and correlated with the depth at which samples were taken. Correlation coefficients were determined by linear regression.

genus *Chloracidobacteria* found on the underside of the ascidian. The relative abundance of *Chloracidobacteria*-associated sequences was generally low but larger in deeper waters ($0.47 \pm 0.38\%$) than in intermediate ($0.43 \pm 0.34\%$) and shallow waters ($0.19 \pm 0.08\%$).

Discussion

Three distinct microhabitats were found associated with *L. patella*, separated by only few millimeters of animal tissue and characterized by steep gradients of the key physicochemical parameters light and O_2. All three microhabitats harbored distinct microbial communities dominated by *Cyanobacteria*. Furthermore, we could correlate the distribution of particular types of microbes to the light and O_2 microenvironment—such correlation is often not done or even impossible in many surveys of microbial diversity because of bulk analysis and/or lack of appropriate metadata. In the following, we discuss these findings in more detail.

Thick tufts of filamentous cyanobacteria containing Chl *a* and phycoerythrin were commonly found lining the opening of the cloacal cavity of *L. patella*, whereas the biofilm community on the underside was heterogeneously distributed and dispersed as distinct clusters often containing Chl *a* and *d* and phycobiliproteins. Functional Chl *d* has thus far only been found in *A. marina*, where it enables the use of NIR for oxygenic photosynthesis. Other ascidian species have previously been shown to host Chl *d*-containing phototrophs (Kühl *et al.*, 2005; López-Legentil *et al.*, 2011; Martínez-García *et al.*, 2011), and even a global distribution of Chl *d*-containing bacteria has been suggested (Kashiyama *et al.*, 2008; Behrendt *et al.*, 2011). Our spectral irradiance measurements demonstrate that NIR is enriched in the cloacal cavity and the underside of *L. patella* as compared with visible light, supporting the occurrence of Chl *d*-containing phototrophs in this optically defined microniche. Similar patterns of NIR enrichment have been observed in coral skeleton (Magnusson *et al.*, 2007) and the underside of other didemnid ascidians, that is, *Diplosoma virens* and *Trididemnum paracyclops* (Kühl *et al.*, 2005; Larkum and Kühl, 2005).

In marine environments, seawater readily attenuates NIR and this attenuation is correlated with water depth and temperature (Pegau and Zaneveld, 1993; Pegau *et al.*, 1997). Interestingly, *A. marina* constitutes one of the largest clusters of OTUs identified from the underside of *L. patella* and we observed a strong negative correlation between *A. marina*-related sequences and sampling depth, suggesting that NIR attenuation through the water column is an important determining factor for the abundance of *A. marina*. This hypothesis is further corroborated by negative correlations of water depth and sequence abundance in the two proteobacterial families *Rhodobacteraceae* and *Rhodospirillaceae*, which contain phototrophs capable of producing Bchl *a* (Ferguson *et al.*, 1987; Imhoff and Hiraishi, 2005). Bchl *a* absorbs further into the infrared part of the spectrum (>800 nm), thus making *Rhodobacteraceae* and *Rhodospirillaceae* even more susceptible to attenuation by seawater. Martinez-Garcia *et al.* (2011) sampled the Mediterranean ascidian *Cystodytes dellechiajei* in shallow waters (<10–23 m) and did not recover sequences related to *A. marina* using denaturing gradient gel electrophoresis. On the contrary, the same study found Chl *d*-like photopigments using fluorescence microscopy on the same ascidians, stressing the possibility for other bacteria as carriers of Chl *d*; how these bacteria then would survive under relatively low NIR concentrations remains unknown. As a side note, it was encouraging to find comparable abundance estimates of Chl *d*-containing phototrophs using both amplicon sequencing in comparison with pigment abundance data from hyperspectral imaging (data not shown, for methodology see Supplementary Online Material).

Additional measurements of scalar irradiance in the cloacal cavity of *L. patella* revealed spectral absorption signatures specific for the photopigments Chl *a*, phycobiliproteins and Bchl *a*, and a strong attenuation of visible light in both the *Prochloron*-containing cloacal cavity and the lowermost tunic-associated biofilm. Ascidian-associated photopigments have been investigated before and essentially all major chlorophylls (Chl *a*, *b*, *c* and *d*) were found present on the surface of the Mediterranean ascidian *C. dellechiajei* (Martínez-García *et al.*, 2011). Recently, a new symbiotic *Acaryochloris* species, *Candidatus* Acaryochloris bahamiensis nov. sp., was found within the tunic of the didemnid ascidian *Lissoclinum fragile*, even demonstrating compartmentalized distribution of Chl *d* and phycobiliproteins within single *A. marina* cells (López-Legentil *et al.*, 2011).

The strong light-scattering effects measured on the surface of *L. patella* with scalar irradiance reaching up to 216% of the incident irradiance is possibly due to reflection by the white spicule-filled tunic commonly produced by didemnid ascidians in combination with light trapping due to a higher refractive index in the tunic as compared with the overlaying water (Kühl and Jørgensen, 1994). Light intensities of up to 280% of incident light have been reported on the surface of microbenthic communities (Kühl and Jørgensen, 1994; Kühl *et al.*, 1994) as well as different types of corals (Kühl and Jørgensen, 1994; Magnusson *et al.*, 2007). The high-light environment found on the surface of *L. patella* presumably selects for phototrophs with appropriate protective mechanisms enabling them to photosynthesize under these conditions.

Oxygen microsensor measurements revealed distinct O_2 microenvironments on and within *L. patella*. Oxygen concentrations within the cloacal

cavity fluctuated from anoxia during darkness to supersaturating conditions during light, whereas the surface biofilm and uppermost tunic remained well oxygenated throughout light and darkness. Oxygen consumption was observed just below the surface of *L. patella*. This O_2 uptake could be due to the animal itself or a bacterial community not recovered by *16S rRNA* gene sequencing, as the inner part of the tunic was not sampled. We observed a rapid decline in O_2 concentration in the cloacal cavity of *L. patella* upon experimental light–dark shifts. Hence, we can hypothesize that the light and O_2 gradients will fluctuate strongly with solar irradiance over the diel cycle. This would present a dynamic microenvironment selecting for specific adaptations in the associated microbial communities (Ley *et al.*, 2006), which may be reflected in the functional groups of associated bacteria and their microbial diversity.

The diversity of bacteria across *L. patella* followed a steep spatial gradient, where three distinct microbial communities were separated by only few millimeters of the ascidian tunic. The microbial community on the underside was highly diverse, with an average Shannon index (*H*) of 6.9 ± 0.2, more variable on the well oxygenated surface (3.3 ± 1.7) and generally much lower within the cloacal cavity of *L. patella* (1.8 ± 0.7). In comparison, marine planktonic habitats exhibited *H* indices ranging from 4.4 to 5.4 (Schloss *et al.*, 2009), whereas temperate coastal microbial mats were found to be slightly more diverse (*H*: 5.9 ± 0.4; Bolhuis and Stal, 2011). Menezes *et al.* (2010) did not calculate *H* indices but still found the bacterial community associated with the didemnid ascidian *D. ligulum* (which is not known to contain *Prochloron*) to be the most diverse of all eight invertebrate species sampled.

Assigning metabolic functions based on *16S rRNA* gene sequences involves some uncertainties but can still provide valuable information on the major metabolisms in microbial communities (Barott *et al.*, 2011; Bolhuis and Stal, 2011). Functionally, the three microhabitats found on *L. patella* were apparently dominated by aerobic bacteria, yet facultative anaerobes were present, most prominently in the cloacal cavity of *L. patella*, where the microenvironment was found to be the most variable in terms of O_2 concentrations, showing rapid shifts between anoxia in darkness and hyperoxia under high irradiance. Sequences associated with obligate anaerobes (genus *Propiogenium)* were found in the well-oxygenated middle section of *L. patella* as well as on the outer surface. Members of the genus *Propiogenium* are known commensals of higher animals capable of growing on succinate, an important end product in anaerobic metabolic processes (Schink and Pfennig, 1982). If *Propiogenium* is truly a genus of only obligate anaerobes, they must exist in permanent anoxic microenvironments within *L. patella*, which even our fine-scale analysis using microsensors was not able to retrieve or, alternatively, such bacteria are able to survive oxic conditions during the day until anoxia at nighttime.

The diversity of microbes and their putative metabolism has been studied in the coral holobiont and associated algae (Barott *et al.*, 2011) and in microbial mats (Bolhuis and Stal, 2011) by use of *16S rRNA* gene sequencing. In comparison with our investigation of *L. patella*, coral-associated algae hosted a similar number of aerobic bacteria (53–94%) but fewer phototrophs (5–32%), whereas corals had almost no phototrophic bacteria associated with them (<1%) and hosted fewer aerobes (Barott *et al.*, 2011). Temperate microbial mats were found to harbor ~30% photoautotrophs consisting of *Cyanobacteria* and photoheterotrophic *Rhodobacterales*, but were otherwise dominated by chemoorganotrophs (Bolhuis and Stal, 2011). Despite the close physical connection of corals and ascidians on coral reefs, their biofilm communities are functionally different and probably the result of adaptation to specific microenvironments or active involvement of the host in shaping the microbial assemblage. However, as the functional assignments in our study are solely based upon conservation of key properties within major taxonomic groups, we are certainly underestimating the real diversity of functional groups that remain hidden in our sequence data.

In terms of sequence abundance, the phyla *Cyanobacteria*, *Proteobacteria* and *Bacteroidetes* were dominating all three microbial communities in *L. patella*, but their relative abundance varied according to sample depth and location. The cloacal cavity of *L. patella* was predominated by sequences belonging to OTUs classified as *Prochloron* spp., a symbiont well known to associate with didemnid ascidians (Lewin, 1981; Lewin and Cheng, 1985). *Prochloron* was first discovered in the early 1970s and received much attention because of its pigment composition (Chl *a* and *b*, absence of phycobiliproteins), which suggested its involvement in chloroplast evolution (Whatley and Whatley, 1981). In 2005, a new class of cytotoxic compounds, patellamides, was found encoded in the *Prochloron* genome (Schmidt *et al.*, 2005), and recently a wide ecological distribution of these gene cassettes was described (Donia *et al.*, 2011). The ecological and functional roles of these compounds remain enigmatic but involvement in metal-detoxification or metal-concentration mechanisms has been suggested (Bertram and Pattenden, 2007). Interestingly, other compounds within the same chemical family, that is, cyanobactins, are toxic to other cyanobacteria, possibly providing *Prochloron* and other cyanobacteria synthesizing such compounds with competitive advantages over other cyanobacteria (Todorova *et al.*, 1995; Jüttner *et al.*, 2001; Hirose *et al.*, 2009). Such allelopathic interactions may explain our finding of only a few other cyanobacteria within the cloacal cavity of *L. patella*.

The cloacal cavity of *L. patella* exhibited dynamic changes in O_2 conditions, with rapid O_2 depletion to anoxia in darkness, potentially conducive to anaerobic processes and bacterial growth. A recent *Prochloron* genome-sequencing effort revealed that the bacterium is heavily involved in nitrogen metabolism, but not in N_2 fixation (Hirose *et al.*, 2009), contrasting previous reports (Paerl, 1984; Kline and Lewin, 1999). We found sequences closely related to the plant rhizosphere bacterium *Azospirillum brasilense* to be a significant part of the microbial community within the cloacal cavity and on the underside of *L. patella*. *A. brasilense* has long been recognized for its capability in terrestrial N_2 fixation (Michiels *et al.*, 1989). Performing N_2-fixation assays on *Prochloron* spp. in the presence of *A. brasilense* or other diazotrophs could thus have caused false-positive results. As a side note, numerous studies have tried to enhance crop production in saline soils using inoculations of *A. brasilense* isolated from high-salinity environments (Nabti *et al.*, 2007, 2010). Our finding of *A. brasilense*-like bacteria in high-salinity seawater could accelerate the search for a halo-tolerant rhizosphere candidate.

Phyla dominating the surface of *L. patella* appear to be following a depth-dependent relationship: Shallow waters apparently promoted the occurrence of *Proteobacteria*, whereas *Cyanobacteria* are dominantly found in deeper waters. Principal component analysis revealed a tight clustering of three surface samples, all originating from shallow water, highlighting the presence of depth-specific bacterial communities. On the surface of *L. patella*, a large proportion of sequences clustered into two large OTUs taxonomically classified as *Planktothricoides* and *Rhodospirillaceae.* The genus *Planktothricoides* contains freshwater cyanobacteria known for their bloom formation and potential toxicity (Suda *et al.*, 2002). *Planktothricoides* has consistently been detected on a Mediterranean ascidian throughout different macroecological conditions and geographic areas (Martínez-García *et al.*, 2011). To our knowledge, only ascidians have been found to harbor *Planktothricoides* in marine environments, suggesting specificity of these surface-associated bacteria on a global scale. *Rhodospirillaceae* (that is, purple non-sulfur bacteria) are known for their capability to perform anoxygenic photosynthesis, owing their distinct color to bacteriochlorophylls and carotenoids (Ferguson *et al.*, 1987). Sequences resembling *Rhodospirillaceae* were predominantly retrieved from ascidians collected in shallow waters, emphasizing their preference for environments with sufficient near infrared-radiation.

Previous studies on ascidian-associated bacterial communities are exemplifying their diversity and geographic specificity. Cyanobacteria were found to be common among epibiotic phototrophs covering the Mediterranean ascidian *C. dellechiajei* (Martínez-García *et al.*, 2011) and within the tunic of Caribbean didemnid ascidians (López-Legentil *et al.*, 2011) but were completely absent in three species of ascidians sampled on the eastern US coast (Tait *et al.*, 2007) and two ascidian species from the north coast of Brazil (Menezes *et al.*, 2010). Bacteria sampled from the tunic tissue and the surfaces of various ascidians revealed sequences belonging to *Proteobacteria*, *Actinobacteria* and *Bacteroidetes* (Martínez-García *et al.*, 2009; Menezes *et al.*, 2010), as well as *Alphaproteobacteria* (Tait *et al.*, 2007), thus closely resembling some of the recovered phyla from *L. patella*.

The bacterial diversity associated with ascidians represents a valuable reservoir in the search for bioactive compounds as well as novel photopigments, and exhibits a large potential in the ongoing search for extremophile bacteria and their use in applied sciences. A thorough description of the biodiversity and microenvironments associated with ascidians may facilitate more efficient cultivation and isolation of novel bacteria from such microhabitats. Combined studies, incorporating analysis of gene expression and microenvironmental measurements, have been performed in microbial mats in hot springs (Steunou *et al.*, 2006, 2008; Jensen *et al.*, 2011), but are otherwise scarce, in particular with respect to large-scale analysis of expression using transcriptome analysis. Relating functional regulation and transcript abundance in a defined and well-described system, such as *L. patella*, could help to elucidate microscale variations of *in situ* microbial metabolism and interactions across microhabitats, further revealing competitive and adaptive mechanisms shaping the microbiome of didemnid ascidians. Our first description of the distinct microhabitats and microbial communities associated with *L. patella* through molecular analysis, imaging and microenvironmental analysis is giving new insights into ascidian-associated bacterial communities and phototrophs in particular, and will help aiding future studies to relate changing microenvironments to functionally relevant adjustments in bacterial communities.

Conclusion

Only a few millimeters of ascidian animal tissue separate three very different microhabitats in *L. patella*, characterized by steep gradients of O_2, light intensity and spectral quality that change dynamically upon changing solar irradiance. In general, all microbial communities associated with these microhabitats in *L. patella* were dominated by cyanobacteria and aerobic bacteria, albeit facultative anaerobes were present, suggesting specific adaptations to the highly variable O_2 conditions in *L. patella* over the diel cycle. Microbial diversity was lowest in the cloacal cavity and highest in biofilms sampled from the underside of the ascidian, reflecting community-wide adaptations to

the physicochemical microenvironments associated with *L. patella*. The biofilm communities harbored conspicuous bacteria including diazotrophs such as *A. brasilense,* inhabiting both the cloacal cavity and the underside of *L. patella*, and the unique Chl *d*-containing cyanobacterium *A. marina.* Sampling of *L. patella* along a depth gradient across the coral reef crest revealed a negative correlation between the abundance of phototrophic bacteria employing NIR (*Rhodospirillaceae*, *Rhodobacteraceae*, *Chloracidobacteria* and *A. marina*) and water depth, indicating that their abundance was strongly influenced by the availability of NIR, which is absorbed by seawater. This first detailed description of the microbial diversity and microhabitats associated with *L. patella* highlights the need to perform such studies at ecologically relevant spatial scales. Both microenvironmental niche-defining parameters and microbial communities can vary significantly over small distances in surface-associated microbial communities, and important knowledge about the structure and function of such communities may be lost in microbial biodiversity surveys of bulk samples with limited metadata.

Acknowledgements

This study was financed by the Danish Natural Science Research Council (MK) and a PhD grant from the Faculty of Science, University of Copenhagen (LB and MIK). We thank the staff at Heron Island Research Station for excellent technical assistance.

References

Adams D. (2002). Symbiotic interactions. In: Whitton B, Potts M (eds). *The Ecology of Cyanobacteria*, 1st edn. Springer: Netherlands, pp 523–561.

Barott KL, Rodriguez-Brito B, Janouškovec J, Marhaver KL, Smith JE, Keeling P *et al.* (2011). Microbial diversity associated with four functional groups of benthic reef algae and the reef-building coral *Montastraea annularis*. *Environ Microbiol* **13**: 1192–1204.

Behrendt L, Larkum AWD, Norman A, Qvortrup K, Chen M, Ralph P *et al.* (2011). Endolithic chlorophyll *d*-containing phototrophs. *ISME J* **5**: 1072–1076.

Bertram A, Pattenden G. (2007). Marine metabolites: metal binding and metal complexes of azole-based cyclic peptides of marine origin. *Nat Prod Rep* **24**: 18–30.

Böer SI, Hedtkamp SIC, van Beusekom JEE, Fuhrman JA, Boetius A, Ramette A. (2009). Time- and sediment depth-related variations in bacterial diversity and community structure in subtidal sands. *ISME J* **3**: 780–791.

Bolhuis H, Stal LJ. (2011). Analysis of bacterial and archaeal diversity in coastal microbial mats using massive parallel 16S rRNA gene tag sequencing. *ISME J* **5**: 1701–1712.

Degnan BM, Hawkins CJ, Lavin MF, McCaffrey EJ, Parry DL, Van den Brenk AL *et al.* (1989). New cyclic peptides with cytotoxic activity from the ascidian *Lissoclinum patella*. *J Med Chem* **32**: 1349–1354.

Donia MS, Fricke WF, Ravel J, Schmidt EW. (2011). Variation in tropical reef symbiont metagenomes defined by secondary metabolism. *PLoS One* **6**: e17897.

Erwin PM, López-Legentil S, Schuhmann PW. (2010). The pharmaceutical value of marine biodiversity for anticancer drug discovery. *Ecol Econ* **70**: 445–451.

Ferguson SJ, Jackson JB, McEwan AG. (1987). Anaerobic respiration in the *Rhodospirillaceae*: characterisation of pathways and evaluation of roles in redox balancing during photosynthesis. *FEMS Microbiol Lett* **46**: 117–143.

Hanna C, Schönberg L, De Beer D, Lawton A. (2005). Oxygen microsensor studies on zooxanthellate clionaid sponges from the Costa Brava, Mediterranean Sea. *J Phycol* **41**: 774–779.

Hirose E, Maruyama T. (2004). What are the benefits in the ascidian-*Prochloron* symbiosis? *Endocytobiosis Cell Res* **15**: 51–62.

Hirose E, Neilan BA, Schmidt EW, Murakami A. (2009). Enigmatic life and evolution of *Prochloron* and related cyanobacteria inhabiting colonial ascidians. In: Gault PM, Marler HJ (eds). *Handbook on Cyanobacteria: Biochemistry, Biotechnology and Applications*, 1st edn. Nova Science Pub Inc., pp 161–189.

Hoffmann F, Røy H, Bayer K, Hentschel U, Pfannkuchen M, Brümmer F *et al.* (2008). Oxygen dynamics and transport in the Mediterranean sponge *Aplysina aerophoba*. *Mar Biol* **153**: 1257–1264.

Holmsgaard PN, Norman A, Hede SC, Poulsen PHB, Al-Soud WA, Hansen LH *et al.* (2011). Bias in bacterial diversity as a result of Nycodenz extraction from bulk soil. *Soil Biol Biochem* **43**: 2152–2159.

Imhoff JF, Hiraishi A. (2005). Aerobic bacteria containing Bacteriochlorophyll and belonging to the *Alphaproteobacteria*. In: Brenner DJ, Krieg NR, Staley JT, Garrity GM (eds). *Bergey's Manual of Systematic Bacteriology*. Vol. 2, 2nd edn. Springer: USA, pp 133–136.

Jensen SI, Steunou A-S, Bhaya D, Kuhl M, Grossman AR. (2011). *In situ* dynamics of O_2, pH and cyanobacterial transcripts associated with CCM, photosynthesis and detoxification of ROS. *ISME J* **5**: 317–328.

Jüttner F, Todorova AK, Walch N, von Philipsborn W. (2001). Nostocyclamide M: a cyanobacterial cyclic peptide with allelopathic activity from Nostoc 31. *Phytochemistry* **57**: 613–619.

Kashiyama Y, Miyashita H, Ohkubo S, Ogawa NO, Chikaraish iY, Takano Y. (2008). Evidence for global chlorophyll *d*. *Science* **321**: 658.

Kline TC, Lewin RA. (1999). Natural N^{-15}/N^{-14} abundance as evidence for N_2 fixation by *Prochloron* (Prochlorophyta) endosymbiotic with didemnid ascidians. *Symbiosis* **26**: 193–198.

Kühl M. (2005). Optical microsensors for analysis of microbial communities. *Meth Enzymol* **397**: 166–199.

Kühl M, Chen M, Ralph PJ, Schreiber U, Larkum AWD. (2005). A niche for cyanobacteria containing chlorophyll *d*. *Nature* **433**: 820.

Kühl M, Cohen Y, Dalsgaard T, Jørgensen BB, Revsbech NP. (1995). Microenvironment and photosynthesis of zooxanthellae in scleractinian corals studied with microsensors for 0_2, pH and light. *Mar Ecol Prog Ser* **117**: 159–172.

Kühl M, Jørgensen BB. (1994). The light field of microbenthic communities: radiance distribution and

microscale optics of sandy coastal sediments. *Limnol Oceanogr* **39**: 1368–1398.

Kühl M, Larkum AWD. (2002). The microenvironment and photosynthetic performance of *Prochloron sp.* in symbiosis with didemnid ascidians. In: Seckbach J (ed). *Cellular origin and life in extreme habitats: Symbioses, mechanisms and model systems*. Vol. 3, 1st edn. Kluwer Academic Publishers: Dordrecht, pp 273–290.

Kühl M, Lassen C, Jørgensen BB. (1994). Light penetration and light intensity in sandy marine sediments measured with irradiance and scalar irradiance fibre-optic microprobes. *Mar Ecol Prog Ser* **105**: 139–148.

Kühl M, Polerecky L. (2008). Functional and structural imaging of phototrophic microbial communities and symbioses. *Aquat Microb Ecol* **53**: 99–118.

Kunin V, Engelbrektson A, Ochman H, Hugenholtz P. (2010). Wrinkles in the rare biosphere: pyrosequencing errors can lead to artificial inflation of diversity estimates. *Environ Microbiol* **12**: 118–123.

Kunin V, Raes J, Harris JK, Spear JR, Walker JJ, Ivanova N *et al.* (2008). Millimeter-scale genetic gradients and community-level molecular convergence in a hypersaline microbial mat. *Mol Syst Biol* **4**: 198.

Larkum AWD, Kühl M. (2005). Chlorophyll *d*: the puzzle resolved. *Trends Plant Sci* **10**: 355–357.

Lewin RA. (1981). Prochloron and the theory of symbiogenesis. *Ann NY Acad Sci* **361**: 325–329.

Lewin RA, Cheng L. (1985). Ecology of Prochloron, a symbiotic alga in ascidians of coral reef areas. *Proc Fifth Int Coral Reef Congress* **5**: 95–101.

Ley RE, Harris JK, Wilcox J, Spear JR, Miller SR, Bebout BM *et al.* (2006). Unexpected diversity and complexity of the Guerrero Negro hypersaline microbial mat. *Appl Environ Microbiol* **72**: 3685–3695.

López-Legentil S, Song B, Bosch M, Pawlik JR, Turon X. (2011). Cyanobacterial diversity and a new Acaryochloris-like symbiont from Bahamian sea-squirts. *PLoS One* **6**: e23938.

Lüdemann H, Arth I, Liesack W. (2000). Spatial changes in the bacterial community structure along a vertical oxygen gradient in flooded paddy soil cores. *Appl Environ Microbiol* **66**: 754–762.

Magnusson SH, Fine M, Kuehl M. (2007). Light microclimate of endolithic phototrophs in the scleractinian corals *Montipora monasteriata* and *Porites cylindrica*. *Mar Ecol Prog Ser* **332**: 119–128.

Martínez-García M, Díaz-Valdés M, Antón J. (2009). Diversity of pufM genes, involved in aerobic anoxygenic photosynthesis, in the bacterial communities associated with colonial ascidians. *FEMS Microbiol Ecol* **71**: 387–398.

Martínez-García M, Koblížek M, López-Legentil S, Antón J. (2011). Epibiosis of oxygenic phototrophs containing chlorophylls *a, b, c* and *d* on the colonial ascidian *Cystodytes dellechiajei*. *Microb Ecol* **61**: 13–19.

Menezes CBA, Bonugli-Santos RC, Miqueletto PB, Passarini MRZ, Silva CHD, Justo MR *et al.* (2010). Microbial diversity associated with algae, ascidians and sponges from the north coast of São Paulo state, Brazil. *Microbiol Res* **165**: 466–482.

Michiels K, Vanderleyden J, Gool A. (1989). *Azospirillum*; plant root associations: a review. *Biol Fertil Soils* **8**: 356–368.

Nabti E, Sahnoune M, Adjrad S, Van Dommelen A, Ghoul M, Schmid M *et al.* (2007). A halophilic and osmotolerant *Azospirillum brasilense* strain from Algerian soil restores wheat growth under saline conditions. *Eng Life Sci* **7**: 354–360.

Nabti E, Sahnoune M, Ghoul M, Fischer D, Hofmann A, Rothballer M *et al.* (2010). Restoration of growth of durum wheat (*Triticum durum* var. waha) under Saline conditions due to inoculation with the Rhizosphere Bacterium *Azospirillum brasilense*; NH and extracts of the marine alga; *Ulva lactuca*. *J Plant Growth Regul* **29**: 6–22-22.

Ogi T, Margiastuti P, Teruya T, Taira J, Suenaga K, Ueda K. (2009). Isolation of C11 cyclopentenones from two didemnid species, *Lissoclinum sp.* and *Diplosoma sp.* *Mar Drugs* **7**: 816–832.

Paerl HW. (1984). N_2 fixation (nitrogenase activity) attributable to a specific Prochloron (Prochlorophyta) -ascidian association in Palau, Micronesia. *Mar Biol* **81**: 251–254.

Pedrós-Alió C. (2006). Marine microbial diversity: can it be determined? *Trend Microbiol* **14**: 257–263.

Pegau WS, Gray D, Zaneveld JRV. (1997). Absorption and attenuation of visible and near-infrared light in water: dependence on temperature and salinity. *Appl Opt* **36**: 6035–6046.

Pegau WS, Zaneveld JRV. (1993). Temperature-dependent absorption of water in the red and near-infrared portions of the spectrum. *Limnol Oceanogr* **38**: 188–192.

Polerecky L, Bissett A, Al-Najjar M, Faerber P, Osmers H, Suci PA *et al.* (2009). Modular spectral imaging system for discrimination of pigments in cells and microbial communities. *Appl Environ Microbiol* **75**: 758–771.

Reeder J, Knight R. (2009). The 'rare biosphere': a reality check. *Nat Meth* **6**: 636–637.

Salomon CE, Faulkner DJ. (2002). Localization studies of bioactive cyclic peptides in the ascidian *Lissoclinum patella*. *J Nat Prod* **65**: 689–692.

Samuel PM. (2000). Developments in aquatic microbiology. *Int Microbiol* **3**: 203–211.

Schink B, Pfennig N. (1982). *Propionigenium modestum* gen. nov. sp. nov. a new strictly anaerobic, nonsporing bacterium growing on succinate. *Arch Microbiol* **133**: 209–216.

Schloss PD, Handelsman J. (2005). Introducing DOTUR, a computer program for defining operational taxonomic units and estimating species richness. *Appl Environ Microbiol* **71**: 1501–1506.

Schloss PD, Westcott SL, Ryabin T, Hall JR, Hartmann M, Hollister EB *et al.* (2009). Introducing mothur: open-source, platform-independent, community-supported software for describing and comparing microbial communities. *Appl Environ Microbiol* **75**: 7537–7541.

Schmidt EW, Nelson JT, Rasko DA, Sudek S, Eisen JA, Haygood MG *et al.* (2005). Patellamide A and C biosynthesis by a microcin-like pathway in *Prochloron didemni*, the cyanobacterial symbiont of *Lissoclinum patella*. *Proc Natl Acad Sci USA* **102**: 7315–7320.

Schreiber U. (2004). Pulse-amplitude-modulation (PAM) fluorometry and saturation pulse method: an overview. Chlorophyll fluorescence: a signature of photosynthesis. Vol. 132, 1st edn. In: Papageorgiou GCG (ed.). Kluwer: Dordrecht, pp 279–319.

Sings HL, Rinehart KL. (1996). Compounds produced from potential tunicate-blue-green algal symbiosis: a review. *J Ind Microbiol Biotechnol* **17**: 385–396.

Sogin ML, Morrison HG, Huber JA, Welch DM, Huse SM, Neal PR *et al.* (2006). Microbial diversity in the deep

sea and the underexplored ''rare biosphere''. *Proc Natl Acad Sci USA* **103**: 12115–12120.

Steunou A-S, Bhaya D, Bateson MM, Melendrez MC, Ward DM, Brecht E *et al.* (2006). *In situ* analysis of nitrogen fixation and metabolic switching in unicellular thermophilic cyanobacteria inhabiting hot spring microbial mats. *Proc Natl Acad Sci USA* **103**: 2398–2403.

Steunou A-S, Jensen SI, Brecht E, Becraft ED, Bateson MM, Kilian O *et al.* (2008). Regulation of nif gene expression and the energetics of N_2 fixation over the diel cycle in a hot spring microbial mat. *ISME J* **2**: 364–378.

Suda S, Watanabe MM, Otsuka S, Mahakahant A, Yongmanitchai W, Nopartnaraporn N *et al.* (2002). Taxonomic revision of water-bloom-forming species of oscillatorioid cyanobacteria. *Int J Syst Evol Microbiol* **52**: 1577–1595.

Swingley WD, Chen M, Cheung PC, Conrad AL, Dejesa LC, Hao J *et al.* (2008). Niche adaptation and genome expansion in the chlorophyll *d*-producing cyanobacterium *Acaryochloris marina*. *Proc Natl Acad Sci USA* **105**: 2005–2010.

Tait E, Carman M, Sievert SM. (2007). Phylogenetic diversity of bacteria associated with ascidians in Eel Pond (Woods Hole, Massachusetts, USA). *J Exp Mar Bio Ecol* **342**: 138–146.

Taylor M, Hill R, Hentschel U. (2011). Meeting report: 1st international symposium on sponge microbiology. *Mar Biotechnol* **13**: 1057–1061.

Taylor MW, Radax R, Steger D, Wagner M. (2007). Sponge-associated microorganisms: evolution, ecology, and biotechnological potential. *Microbiol Mol Biol Rev* **71**: 295–347.

Thomas TRA, Kavlekar DP, LokaBharathi PA. (2010). Marine drugs from sponge-microbe association-a review. *Mar Drugs* **8**: 1417–1468.

Todorova AK, Juettner F, Linden A, Pluess T, von Philipsborn W. (1995). Nostocyclamide: a new macrocyclic, thiazole-containing allelochemical from *Nostoc sp.* 31 (cyanobacteria). *J Org Chem* **60**: 7891–7895.

Trampe E, Kolbowski J, Schreiber U, Kühl M. (2011). Rapid assessment of different oxygenic phototrophs and single-cell photosynthesis with multicolour variable chlorophyll fluorescence imaging. *Mar Biol* **158**: 1667–1675.

Ward DM, Bateson, M. M., Ferris MJ, Kühl M, Wieland A *et al.* (2006). Cyanobacterial ecotypes in the microbial mat community of Mushroom Spring (Yellowstone National Park, Wyoming) as species-like units linking microbial community composition, structure and function. *Philos Trans R Soc B Biol Sci* **361**: 1997–2008.

Webster NS, Taylor MW. (2011). Marine sponges and their microbial symbionts: love and other relationships. *Environ Microbiol*; e-pub ahead of print 28 March 2011; doi:2010.1111/j.1462-2920.2011.02460.x.

Whatley JM, Whatley FR. (1981). Chloroplast evolution. *New Phytol* **87**: 233–247.

Youngseob Y, Changsoo L, Jaai K, Seokhwan H. (2005). Group-specific primer and probe sets to detect methanogenic communities using quantitative real-time polymerase chain reaction. *Biotechnol Bioeng* **89**: 670–679.

Supplementary Information accompanies the paper on The ISME Journal website (http://www.nature.com/ismej)